HETEROCYCLES, Vol. 106, No. 6, 2023, pp. -. © 2023 The Japan Institute of Heterocyclic Chemistry
Received, 27th February, 2023, Accepted, 7th April, 2023, Published online, 12th April,2023
DOI: 10.3987/COM-23-14833

# *N*-ALKYLATION OF AZOLES WITH ENONES ASSISTED BY P(III) OR $Fe_2O_3$-NANOPARTICLES AS RECYCLABLE CATALYST

**Elangbam Pinky Devi,[a] Saibabu Polina,[b] Kamal Kant,[a] Arup K. Kabi,[c] Nabil Al-Zaqri,[d] Nayyef Aljaar,[e] and Chandi C. Malakar[a]***

[a] Department of Chemistry, National Institute of Technology Manipur, Langol, Imphal-795004, Manipur, India. E-mail: chdeepm@gmail.com, cmalakar@nitmanipur.ac.in

[b] Department of Chemistry, CHRIST (Deemed to be University), Bangalore - 560029, India.

[c] Department of Chemistry, Sungkyunkwan University, Suwon, 16419 Korea.

[d] Department of Chemistry, College of Science, King Saud University, P.O. Box 2455, Riyadh, 11451, Saudi Arabia.

[e] Department of Chemistry, Faculty of Science, The Hashemite University, P.O. Box 330127, Zarqa 13133, Jordan.

**Abstract** – Hexamethylphosphorous triamide (HMPT)-assisted and $Fe_2O_3$-nanoparticles (NPs) catalysed approaches towards the formation of C-N bond is described by the reaction between azoles and enone-compounds. The transformations were accomplished under mild conditions at temperatures 25 °C and 50 °C respectively. The efficacy and robustness of the reaction conditions can be envisioned by regioselective construction of *N*-heterocyclic scaffolds embedded with cycloalkyl residue. The established reaction conditions were found competent over a series of enones and azole derivatives to furnish the desired molecules in high yields ranging from 52-86% under P(III)-mediated conditions and 67-86% under the influences of $Fe_2O_3$-NPs as recyclable catalyst. It was observed that the catalyst can be recycled up to six times with good yields of the product.

The recognition of cycloalkyl-substituted *N*-heterocyclic moieties can be realized by their ubiquitous appearances in diversity of bioactive molecules.[1] Importance of these moieties was further witnessed by

their occurrences in modern drugs such as phosphoinositide 3-kinase (PI3K) inhibitors,[1a] epidermal growth factor receptor (EGFR) inhibitors,[1b] cilostazol (to treat peripheral vascular disease),[1c] cytochrome P450 (CYP) 17 inhibitors anti-androgens,[1d] interleukin-1 receptor-associated kinases (IRAKs) inhibitors[1e] (Figure 1). These heterocyclic skeletons were prepared by C-N bond formation approach. In the area of C-N bond formation, the traditionally employed strategy such as aza-Michael protocol holds an important position owing to its advantage over other methodologies. Nevertheless, the preferences of adding azoles to cyclic enones were hindered by the structural complexities of cyclic enones and due to the low nucleophilicity of azoles.[2] According to earlier reported methods, a series of reagents such as metals,[3] bases,[4] organocatalysts,[5] inorganic supports,[6] lanthanides,[7] fluorides,[8] and enzymes[9] have been widely explored to accomplish aza-Michael addition reactions. These transformations were also described under catalyst-free conditions and Brønsted acid-induced conditions, which are operated under harsh conditions at high pressure to deliver unselective product formation.[10,11] Nonetheless, it is noteworthy to mention that the reactions of cyclic enone derivatives with azole molecules using aza-Michael addition approach are rarely explored.[2a,6b,11]

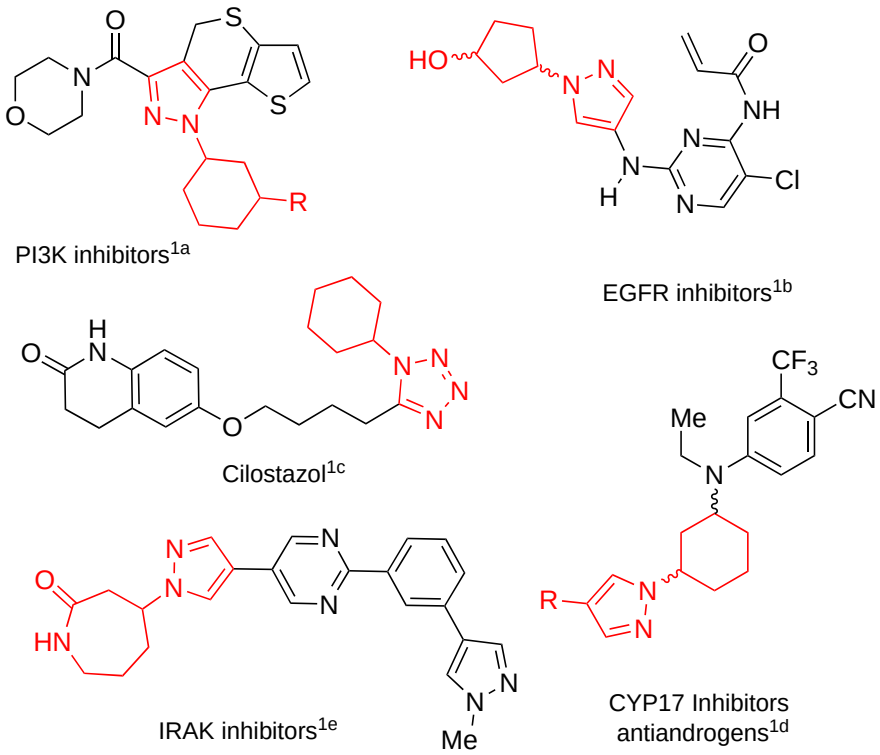


**Figure 1.** *N*-Cycloalkyl azoles containing drug molecules

Recently, a T3P-mediated approach has been described for the reaction of enone-molecules with diverse azoles employing aza-Michael addition protocol at room temperature with good yields and selectivity.[12] Additionally, during the past decades, the greener approaches of Michael-addition reaction have accumulated increasing interest and found enormous application in organic synthesis.[3-5,7,11] In this regard,

we have designed a new process by utilizing a mild and robust HMPT as reagent for the reaction between enones and azoles at room temperature. On the other hand, iron oxides have been witnessed as practical and competent material for a series of organic transformations with excellent catalytic activities.[13] Moreover, the environmental benign and cheap iron catalysts extend the scope in industrial-scale synthesis of numerous fine chemicals and remain considerable for the development of novel synthetic processes. In this regard, we have employed catalytic amounts of $Fe_2O_3$-nanoparticles ($Fe_2O_3$-NPs) as recyclable catalyst for the reaction of cyclic enones with azoles (Scheme 1).

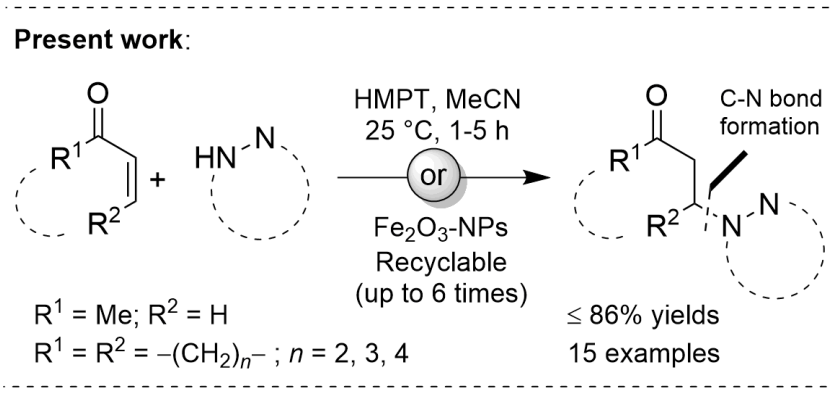


**Scheme 1.** Our method for the preparation of *N*-cycloalkyl azole derivatives

The experimental studies were initiated by considering 2-cyclohexen-1-one **1a** and 1*H*-indazole **2g** as initial starting materials for the optimization studies. The model substrate 1*H*-indazole **2g** has been employed in the screening experiments to reveal the reactivity of azole derivatives embedded with aromatic ring. To begin with, the reaction between substrates **1a** and **2g** was screened under various organophosphorus compounds such as $P^nBu_3$, $PPh_3$, hexamethylphosphoramide (HMPA) and HMPT (Table 1, entries 1-4). It was noted that except HMPT (entry 4), all tested phosphorus reagents (entries 1-3) failed to affect the desired chemical transformation and HMPT as reagent delivered the product **3ag** in 78% yield. Reactions in the presence of phosphines might lead to the formation of deoxygenated side products and unwanted intermediates, and thereby these transformations resulted in a mixture of undesired side products, in which the formation of the required compounds were restricted. In case of HMPA, due to the presence of pentavalent phosphorus the reaction is not effective. Inspired by these results, we intended to consider HMPT as reagent for further optimization to obtain improved yields. Next, we examined the influences of the amount of HMPT and it was found that the variations in reagent loading could not enhance the yield of product **3ag** (entries 5-7). Next, we examined the effects of solvents on reaction yields. The screened solvents such as EtOAc, MeOH, $Et_2O$, 1,4-dioxane and $CH_2Cl_2$ have not exhibited better yields of the product (entries 8-12). Solvents like EtOAc and MeOH were less

active, which might be due to the reaction of these solvents with the phosphorus atom of HMPA. This effect may be slightly diminished when ether solvents like $Et_2O$ and 1,4-dioxane were employed. Further, the alteration of the reaction temperature and time furnishes inadequate outcome of the reaction (entries 13-15). On the other hand, under solvent-free conditions only 29% of the product **3ag** can be observed with unreacted starting materials (entry 16). Having developed the P(III)-mediated homogeneous conditions, we next focused on the investigation of recyclable heterogeneous catalytic system for this transformation. To achieve this purpose, 10 mol% of $Fe_2O_3$-nanoparticles ($Fe_2O_3$-NPs) were used as catalyst for the reaction between **1a** (1.0 mmol) and **2g** (1.0 mmol) in MeCN at 25 °C for 2 hours. Interestingly, it was found that the product **3ag** can be isolated in 31% yield (entry 17). In order to enhance the formation of product **3ag**, the reaction temperature and time was increased (entries 18-20), and observed that the yield of product can be maximized up to 76% at 50 °C in 5 hours of reaction time. After effective screening of suitable conditions for this transformation, we have established that the performed reaction between **1a** (1.0 mmol) and **2g** (1.0 mmol) in the presence of 1.1 equiv. of HMPT using MeCN as solvent at 25 °C delivered highest yield (78%) of the product **3ag** in 2 hours (entry 4, **Conditions A**). On the other hand, under heterogeneous conditions the maximum yield (81%) of the product was achieved, when the reaction was performed using 10 mol% $Fe_2O_3$-NPs in MeCN at 50 °C for 5 hours (entry 20, **Conditions B**).

**Table 1.** Optimization of reaction conditions for the reaction of **1a** with **2g**[a]

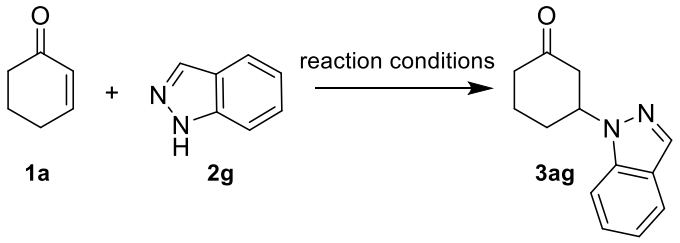


| Entry | Reagent (equiv.) | Solvent | t (h)/ T (°C) | %Yield **3ag**[b] |
|---|---|---|---|---|
| 1 | $P^nBu_3$ (1.1) | MeCN | 2 / 25 | 0 |
| 2 | $PPh_3$ (1.1) | MeCN | 2 / 25 | 0 |
| 3 | HMPA (1.1) | MeCN | 2 / 25 | <10 |
| 4 | HMPT (1.1) | MeCN | 2 / 25 | 78 |
| 5 | HMPT (1.5) | MeCN | 2 / 25 | 76 |
| 6 | HMPT (0.5) | MeCN | 2 / 25 | 46 |
| 7 | - | MeCN | 2 / 25 | 0 |
| 8 | HMPT (1.1) | EtOAc | 2 / 25 | 58 |
| 9 | HMPT (1.1) | MeOH | 2 / 25 | 31 |
| 10 | HMPT (1.1) | $Et_2O$ | 2 / 25 | 60 |

| | | | | |
|---|---|---|---|---|
| 11 | HMPT (1.1) | dioxane | 2 / 25 | 63 |
| 12 | HMPT (1.1) | $CH_2Cl_2$ | 2 / 25 | 71 |
| 13 | HMPT (1.1) | MeCN | 2 / 50 | 59 |
| 14 | HMPT (1.1) | MeCN | 1 / 25 | 46 |
| 15 | HMPT (1.1) | MeCN | 4 / 25 | 69 |
| 16 | HMPT (1.1) | - | 3 / 25 | 29[c] |
| 17 | $Fe_2O_3$ (0.1) | MeCN | 2 / 25 | 31 |
| 18 | $Fe_2O_3$ (0.1) | MeCN | 2 / 50 | 43 |
| 19 | $Fe_2O_3$ (0.1) | MeCN | 2 / 80 | 57 |
| 20 | $Fe_2O_3$ (0.1) | MeCN | 5 / 50 | 81 |
| [a] Reactions were carried out by employing **1a (**1.0 mmol) and **2g** (1.0 mmol) in solvent (2 mL). [b] Indicates the isolated yields. [c] Starting materials remain unreacted. | | | | |

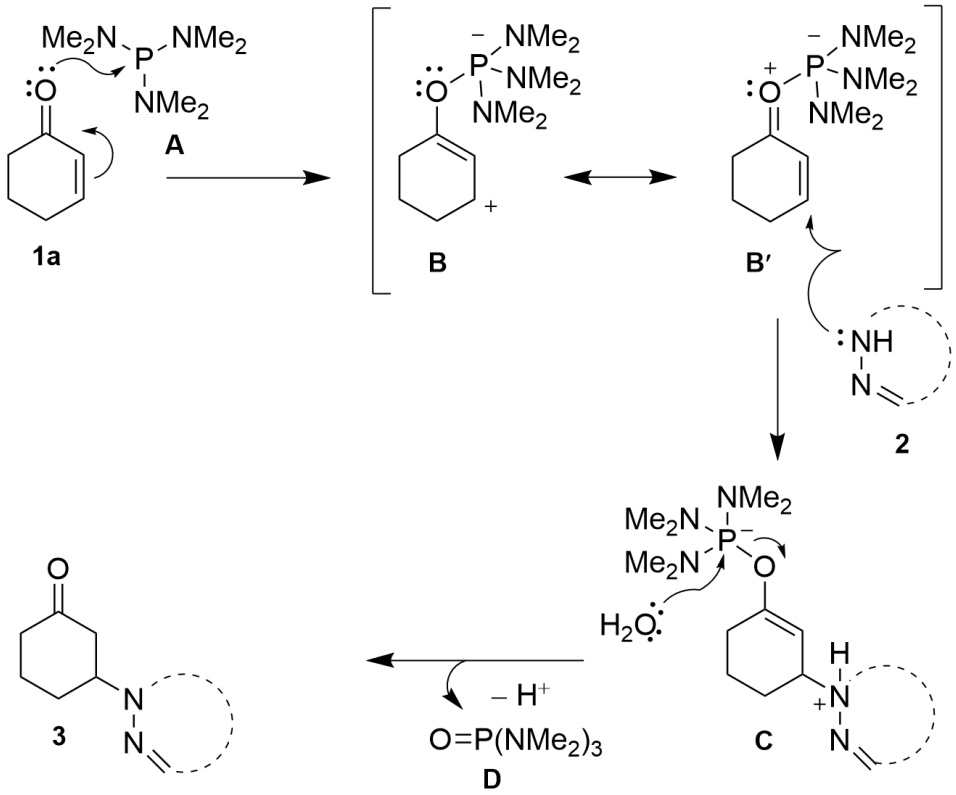


**Scheme 2.** Plausible mechanistic pathway for the $P(NMe_2)_3$-assisted addition reaction of azoles to enones.

After establishing the optimized conditions for the envisaged transformation, we focused on proposing a plausible mechanistic pathway under the HMPT-mediated conditions for the synthesis of desired products (Scheme 2).[12,14] The electron pair situated on oxygen atom of enone **1a** may participate in nucleophilic attack towards the phosphorus atom of $P(NMe_2)_3$ (**A**), which leading to the formation of expected intermediate **B** and that may be assumed in the existence of resonance form **B′**. The reaction between

intermediate **B′** and azole **2** could deliver the intermediate **C**, which finally produces the expected molecule **3** followed by consequent hydrolysis of P-O bond and tautomerization process. The developed transformation produces 1,4-addition products as preferred regio-isomers over 1,2-addition products, which may be associated to the less nucleophilic character of azole derivatives that favours the addition *via* Michael reaction.

With these optimized conditions, we have evaluated the competency of this transformation with a series of azole molecules **2a-i** (Scheme 3). It was observed that when HMPT reagent is employed (**Conditions A**) the pyrazole derivatives **2a**-**e** undergo aza-Michael reaction satisfactorily by delivering the desired products **3aa**-**ae** in adequate yields; whereas, the nitro-group containing pyrazole molecule **2d** leading to the generation of the product in moderate yield (52%). Furthermore, it was found that when 1,2,4-triazole derivative **2f** was exposed under the standard conditions, the single regio-isomer **3af** was obtained in 76% yield. The regioselective formation of compounds **3ab**, **3ac**, **3ae** and **3af** can be explained by more extent of electron density on $N^1$-atom than other N-atoms in the five-membered ring, which makes $N^1$-atom to participate in the nucleophilic attack. Next, it has been described that the indazoles **2g-i** with substitution and without substitution cooperated excellently when reacted under standard reaction conditions and leading to the regioselective synthesis of desired compounds in satisfactory isolated yields. The substrate scope of this method was then examined using $Fe_2O_3$-NPs as recyclable catalyst (**Conditions B**). It has been observed that the azole derivatives **2a-i** have reacted smoothly under the developed conditions to furnish the desired molecules **3aa**-**3ai** in similar yields. Under these conditions the yield of product **3ad** has also been improved up to 67%. It has been described that a series of azoles like pyrrazole and indazole derivatives containing electron neutral (-H) and electron donating functional groups (-Me) derived the products in slightly better yields than that of azoles containing electron withdrawing groups such as $-CF_3$, $-NO_2$, $-CO_2Me$, and -Br. The decreased yields of the products with electron-deficient molecules may be explained by their less nucleophilic abilities. Thus, it was concluded that a spectrum of functional groups on azoles were tolerated well under both developed reaction conditions to produce *N*-heterocyclic (pyrrazole and indazole) scaffolds embedded with cycloalkyl residue (Scheme 3).

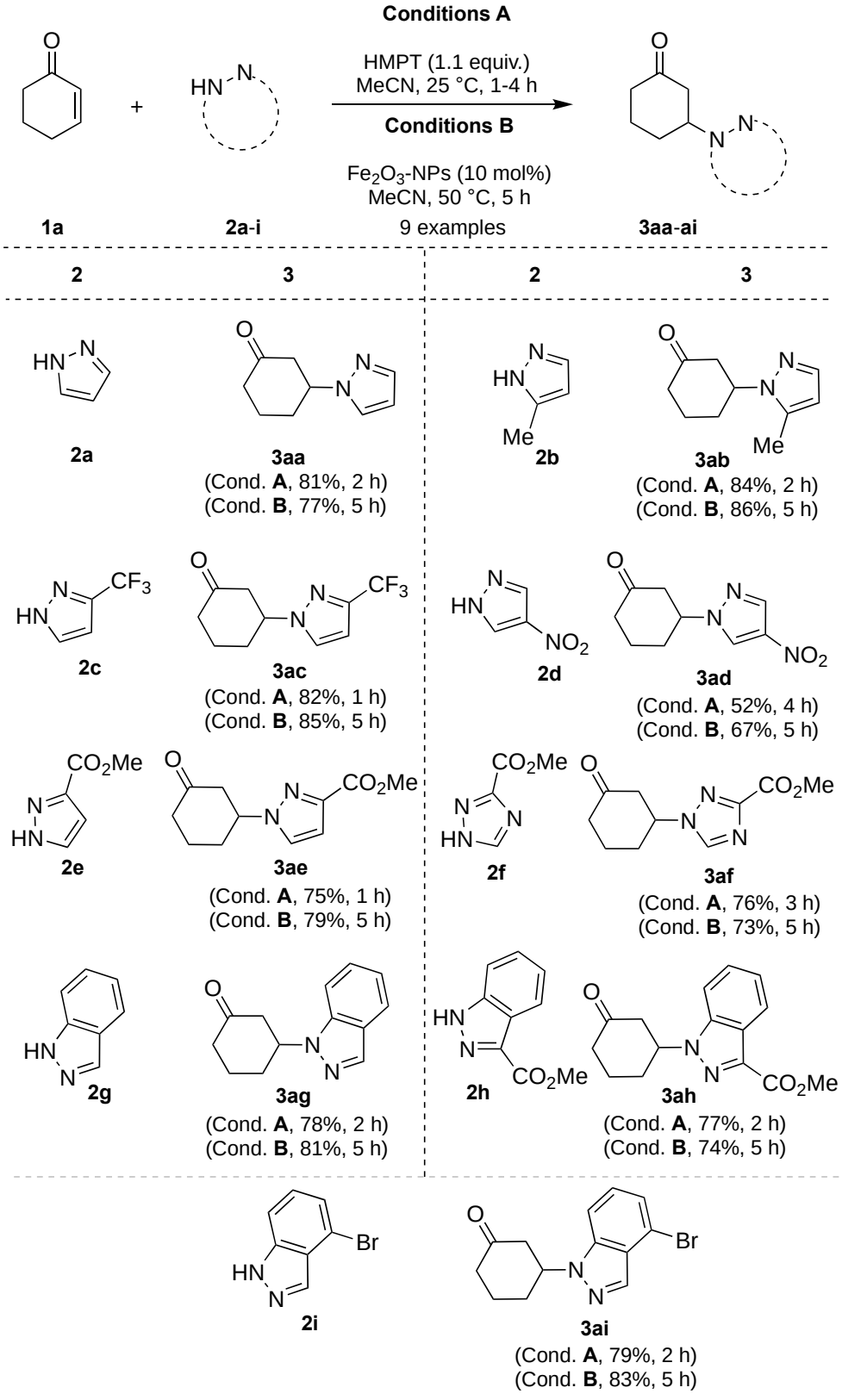


**Scheme 3.** Diversity of azole derivatives for the developed transformation

Next, we have executed reactions between diverse enone derivatives **1b-d** and different azole molecules **2a**, **g**-**h** under described conditions **A** and **B**, which acknowledged the delivery of expected compounds

**3ba-g**, **ca**, **cg-h**, **dg** in high yields (74%-87%) and selectivity (Scheme 4). Under these conditions, enone derivatives of ring size five to seven membered were smoothly reacted including the acyclic enone compound to derive the product.

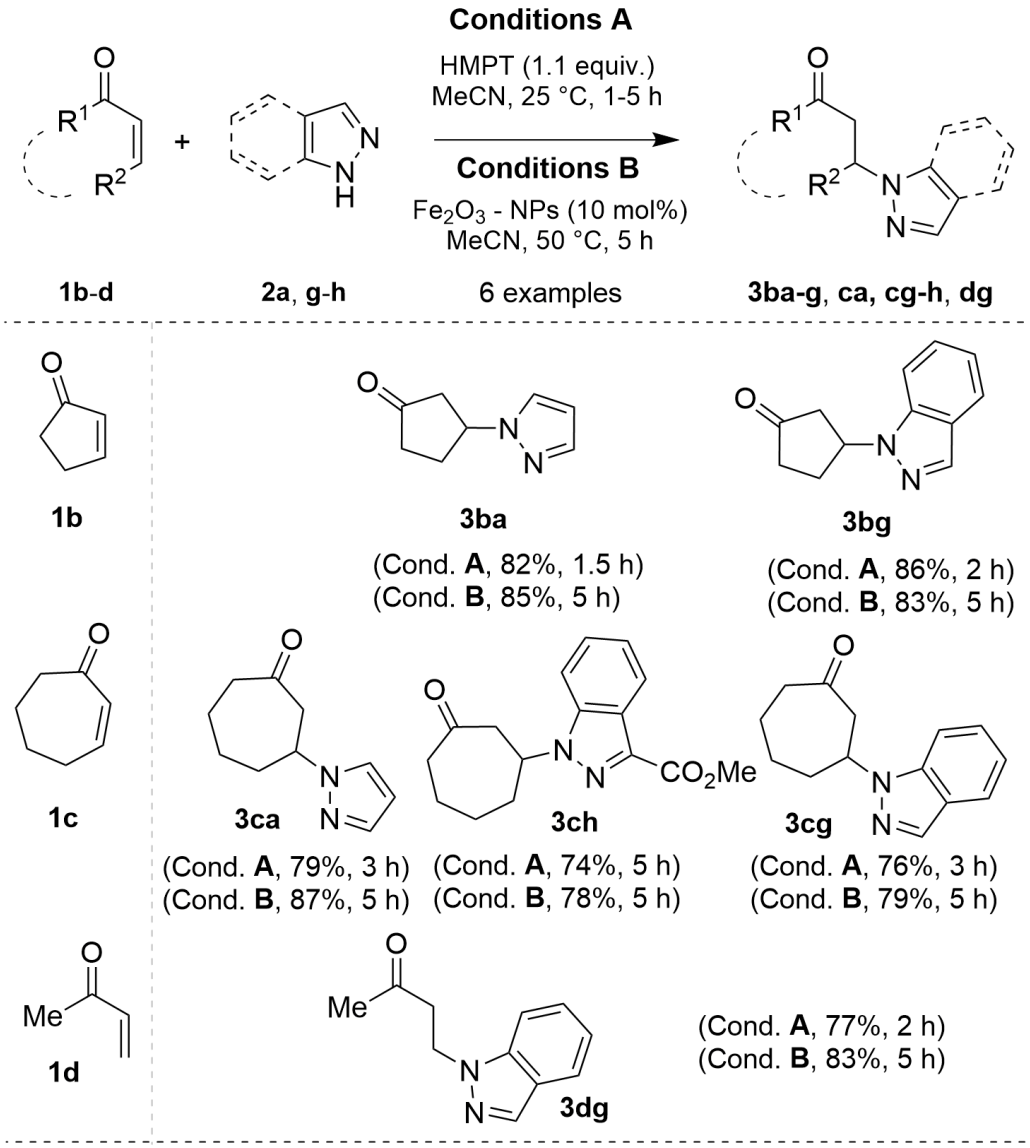


**Scheme 4.** Variation of enones for the developed transformation

To explain the plausible mechanism, it can be stated the catalyst $Fe_2O_3$-NPs exerts the Lewis acidic activities to coordinate with carbonyl group of enone derivatives **1a**, which lead to the formation of complex **A**. Then, the nucleophilic attack of azole derivatives **2** could deliver the desired products **3** in high yields (Scheme 5).

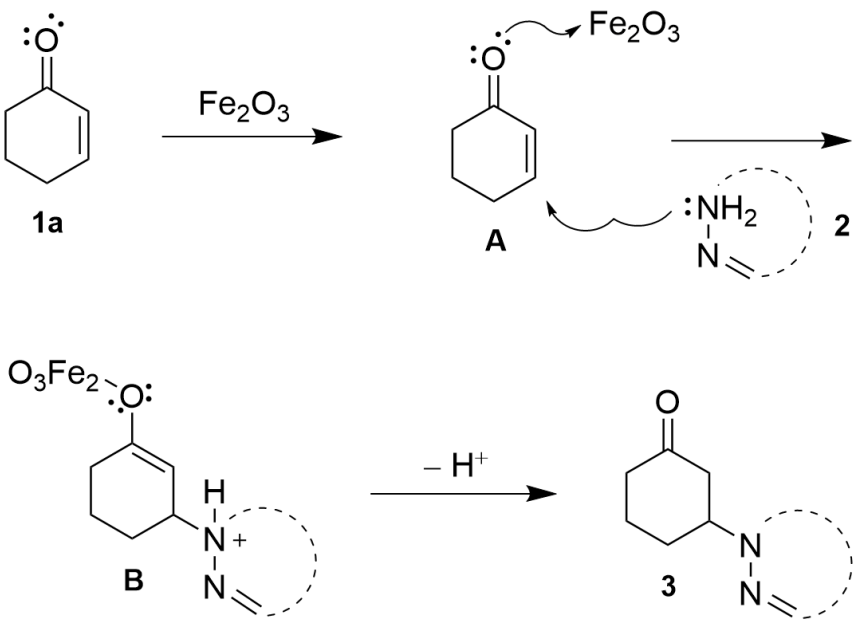


**Scheme 5.** Plausible mechanistic pathway for $Fe_2O_3$-NPs assisted reaction between azoles and enones

After successful development of catalytic activity of $Fe_2O_3$-NPs, we have attempted to investigate the recycling performances of the ferrite nanoparticles. When the reaction was completed, the catalyst was isolated by the process of centrifugation. The reaction mixture was exposed towards the extraction process to obtain the product. The isolated $Fe_2O_3$-NPs was cleansed with EtOAc, dried under vacuum and employed for next cycle of reaction without any reactivation or purification process. It was described that the $Fe_2O_3$-NPs can be employed up to 6 runs as effective catalyst to obtain the product **3** in yields ranging from 71%-78%.

Overall, the developed P(III)-mediated method addresses a series of advantages over previous reported protocols such as better reaction yields, lower reaction time and selectivity in the product formation. Moreover, the previous reported approaches rely on the homogeneous reaction mixture and hence, the associated complexity towards recovery of reagents or catalysts remain challenging exercise. In this regard, the investigated heterogeneous $Fe_2O_3$-NPs catalysed method lead to the formation of products in similar yields and selectivity, and could find broader application due to catalyst recovery without loss of the catalytic activity, which represent these protocols as preferable over other methods.

## CONCLUSION

In summary, a robust $P(NMe_2)_3$-directed reaction between azoles and enones is described for the preparation of *N*-cycloalkyl moieties *via* C-N bond forming reactions. The application of this transformation is further verified by employing heterogeneous catalysis under the influences of $Fe_2O_3$-NPs. The developed strategy lead to excellent substrate scope and catalyst recycling abilities up to

six runs without considerable loss of catalytic activities. The desired molecules were acquired with good selectivity and excellent yields up to 86% yields.

## EXPERIMENTAL

All substrates and reagents were procured from commercial suppliers (Alfa-Aesar, Sigma-Aldrich, Merck, SD fine chemicals, HI Media) and were utilized without prior purification, unless otherwise indicated. All reactions were conducted in 10 mL round bottom flask with magnetic stirring. Solvents employed in purification and extraction were distilled prior to use. Thin-layer chromatography (TLC) was carried-out on TLC plates availed from Merck. Compounds were observed by immersion in $KMnO_4$ staining solution followed by heating or with UV light ($\lambda$ = 254 nm). $^1H$ ($^{13}C$) NMR spectra were recorded in 400 (100) MHz on Brucker spectrometer using $CDCl_3$ and DMSO-$d_6$ as solvents. The $^1H$ and $^{13}C$ chemical shifts were referenced to residual solvent signals at $\delta_{H/C}$ 7.26/77.28 ($CDCl_3$) and $\delta_{H/C}$ 2.51/39.50 (DMSO-$d_6$) relative to TMS as internal standard. Coupling constants *J* [Hz] were directly taken from the spectra and are not averaged. Splitting patterns are designated as s (singlet), d (doublet), t (triplet), q (quartet), m (multiplet), overlapped and br (broad). Products were purified by CombiFlash MPLC. All HRMS spectra are recorded using 6545 QTOF LC/MS, Agilent instrument equipped with an auto sampler in EI-QTOF method in MeCN.

**Synthesis of Hematite iron oxide ($\alpha$-$Fe_2O_3$) nanoparticles**: Hematite iron oxide ($\alpha$-$Fe_2O_3$) nanoparticles are obtained from starting $Fe(NO_3)_3$ (2.0 g, 8.3 mmol) using auto-combustion method. The $Fe(NO_3)_3$ is mixed in distilled $H_2O$ (100 mL), then 3.0 equivalents of glycine (1.86 g, 24.5 mmol) was added in the solution and heated at 100 °C for 1 h. The amino acid glycine assists during chelation and combustion process. Temperature of the reaction mass is excelled up to 150 °C to induce the auto-combustion process. The glycine and $NO_3^-$ ion act as reducing and oxidizing agents, and these assist in thermally induced redox reaction. The auto-combustion process lead to the release of excessive amounts of heat that transform Fe(III)-glycine complex into dried $Fe_2O_3$ particles, which is then calcined at 600 °C for 2 h to achieve 1.0 g of the crystalline hematite $Fe_2O_3$ particles with 80% yield.

### General Experimental Procedure for the Synthesis of Products 3aa-ai and 3ba, bg, ca, cg, ch, dg using HMPT

A 10 mL round bottom flask was charged with enones **1a-d** (1.0 mmol), azoles **2a-i** (1.0 mmol) in MeCN (2 mL), then $P(NMe_2)_3$ (1.1 mmol) was added and the reaction mixture was stirred at room temperature (25 °C) for 1-5 h. After completion of the reaction (progress was monitored by TLC; $SiO_2$, Hexane/EtOAc = 8:2 and LC-MS), the mixture was quenched with saturated aq. $NaHCO_3$ solution,

diluted with water (20 mL) and extracted with EtOAc (3 × 15 mL). The combined organic layers were dried over anhydrous $Na_2SO_4$. Solvent was removed under reduced pressure and the remaining residue was purified over CombiFlash MPLC using Hexane/EtOAc = 80:20 as an eluent to obtain the desired aza-Michael addition products **3aa-ai** and **3ba**, **bg**, **ca**, **cg**, **ch**, **dg** in high yields.

**General Experimental Procedure for the Synthesis of Products 3aa-ai and 3ba, bg, ca, cg, ch, dg using $Fe_2O_3$ nanoparticles as Recyclable Catalyst**

A 10 mL round bottom flask was charged with enones **1a-d** (1.0 mmol), azoles **2a-i** (1.0 mmol) in MeCN (2 mL), then $Fe_2O_3$ nanoparticles (0.1 mmol) was added and the reaction mixture was stirred at 50 °C for 5 hours. After completion of the reaction (progress was monitored by TLC; $SiO_2$, Hexane/EtOAc = 8:2 and LC-MS), the catalyst was isolated by the process of centrifugation. The reaction mixture was exposed towards the extraction process to obtain the crude product, which was purified by column chromatography. The isolated $Fe_2O_3$-NPs was cleansed with EtOAc, dried under vacuum and employed for next cycle of reaction without any reactivation or purification process.

**Analytical Data of Synthesized aza-Michael Addition Products 3aa-ai and 3ba, bg, ca, cg, ch, dg:**

**3-(1*H*-Pyrazol-1-yl)cyclohexanone (3aa)**[12] (Scheme 3): Brown liquid; $R_f$ = 0.60 ($SiO_2$, Hexane/EtOAc = 8:2); purification system: CombiFlash MPLC (Hexane/EtOAc = 80:20); $^1$H NMR (400 MHz, $CDCl_3$) δ = 7.54 (br, 1H), 7.4 (d, *J* = 1.2 Hz, 1H), 6.25 (br, 1H), 4.58-4.51 (m, 1H), 3.03-2.95 (dd, *J* = 14.5, 10.0 Hz, 1H), 2.85-2.8 (dd, *J* = 14.5, 5.0 Hz, 1H), 2.48-2.4 (m, 2H), 2.28-2.24 (m, 2H), 2.10-2.03 (m, 1H), 1.8-1.68 (m, 1H) ppm; $^{13}$C NMR (100 MHz, $CDCl_3$): δ = 207.8, 139.3, 127.4, 105.3, 59.7, 47.6, 40.6, 31.7, 21.7 ppm; HRMS (EI-QTOF, $[M + H]^+$): calculated for $C_9H_{13}N_2O$: 165.1027; found: 165.1024.

**3-(5-Methyl-1*H*-pyrazol-1-yl)cyclohexanone (3ab)**[12] (Scheme 3): Pale yellow liquid; $R_f$ = 0.60 ($SiO_2$, Hexane/EtOAc = 8:2); purification system: CombiFlash MPLC (Hexane/EtOAc = 80:20); $^1$H NMR (400 MHz, $CDCl_3$) δ = 7.26 (d, *J* = 1.6 Hz, 1H), 6.0 (d, *J* = 1.6 Hz, 1H), 4.45-4.36 (dt, *J* = 14 Hz, 1H), 2.96 (dd, *J* = 14.0 Hz, 10.4 Hz, 1H), 2.8 (dd, *J* = 14.4 Hz, 5.0 Hz, 1H), 2.45 (t, *J* = 7.8 Hz, 1H), 2.27 (s, 3H), 2.23 (d, *J* = 4.8 Hz, 2H), 2.07-2.0 (m, 1H), 1.75-1.57 (m, 1H) ppm; HRMS (EI-QTOF, $[M + H]^+$): calculated for $C_{11}H_{15}N_2O$: 191.1184; found: 191.1181.

**3-(3-(Trifluoromethyl)-1*H*-pyrazol-1-yl)cyclohexanone (3ac)**[12] (Scheme 3): Pale brown sticky liquid; $R_f$ = 0.60 ($SiO_2$, Hexane/EtOAc = 8:2); purification system: CombiFlash MPLC (Hexane/EtOAc = 80:20); $^1$H NMR (400 MHz, $CDCl_3$) δ = 7.45 (d, *J* = 1.6 Hz, 1H), 6.5 (d, *J* = 1.6 Hz, 1H), 4.60-4.52 (m, 1H), 3.0 (dd, *J* = 14.0 Hz, 10.4 Hz, 1H), 2.87 (dd, *J* = 14.4 Hz, 4.8 Hz, 1H), 2.50-2.41 (m, 2H), 2.31-2.27 (m, 2H), 2.1-2.04 (m, 1H), 1.78-1.68 (m, 1H) ppm; $^{13}$C NMR (100 MHz, $CDCl_3$): δ = 207.0, 142.5 (q, *J* =

38.0 Hz), 128.9, 121.2 (q, *J* = 267.3 Hz) 104.2, 60.6, 47.4, 40.4, 31.5, 21.6 ppm; HRMS (EI-QTOF, [M + H]$^+$): calculated for $C_{10}H_{12}F_3N_2O$: 233.0901; found: 233.0900.

**3-(4-Nitro-1*H*-pyrazol-1-yl)cyclohexanone (3ad)**[12] (Scheme 3): Grey Solid; $R_f$ = 0.60 ($SiO_2$, Hexane/EtOAc = 8:2); purification system: CombiFlash MPLC (Hexane/EtOAc = 80:20); m.p = 131-133 °C; $^1$H NMR (400 MHz, $CDCl_3$) δ = 7.48 (s, 1H), 6.9 (s, 1H), 4.6-4.53 (m, 1H), 3.02 (dd, *J* = 14.0 Hz, 10.4 Hz, 1H), 2.87 (dd, *J* = 14.4 Hz, 4.9 Hz, 1H), 2.51-2.4 (m, 2H), 2.4-2.32 (m, 2H), 2.16-2.07 (m, 1H), 1.8-1.57 (m, 1H) ppm; $^{13}$C NMR (100 MHz, $CDCl_3$): δ = 206.2, 130.4, 102.8, 61.6, 47.1, 40.3, 31.4, 21.6 ppm; HRMS (EI-QTOF, [M + H]$^+$): calculated for $C_9H_{12}N_3O_3$: 210.0878; found: 210.0873.

**Methyl 1-(3-oxocyclohexyl)-1*H*-pyrazole-3-carboxylate (3ae)**[12] (Scheme 3): Pale brown liquid; $R_f$ = 0.60 ($SiO_2$, Hexane/EtOAc = 8:2); purification system: CombiFlash MPLC (Hexane/EtOAc = 80:20); $^1$H NMR (400 MHz, $CDCl_3$) δ = 7.43 (d, *J* = 2.0 Hz, 1H), 6.8 (d, *J* = 2.0 Hz, 1H), 4.6-4.53 (m, 1H), 3.9 (s, 3H), 3.02 (dd, *J* = 14.4 Hz, 10.0 Hz, 1H), 2.85 (dd, *J* = 14.0 Hz, 5.0 Hz, 1H), 2.47-2.38 (m, 2H), 2.3-2.26 (m, 2H), 2.1-2.03 (m, 1H), 1.78-1.66 (m, 1H) ppm; $^{13}$C NMR (100 MHz, $CDCl_3$): δ = 207.1, 162.6, 143.6, 128.9, 108.9, 60.9, 52.0, 47.5, 40.4, 31.6, 21.8 ppm; HRMS (EI-QTOF, [M + H]$^+$): calculated for $C_{11}H_{15}N_2O_3$: 223.1082; found: 223.1078.

**Methyl 1-(3-oxocyclohexyl)-1*H*-1,2,4-triazole-3-carboxylate (3af)**[12] (Scheme 3): White solid; $R_f$ = 0.5 ($SiO_2$, Hexane/EtOAc = 8:2); purification system: CombiFlash MPLC (Hexane/EtOAc = 80:20); mp = 124-125 °C (Lit[1] mp = 122.4-123.6 °C); $^1$H NMR (400 MHz, DMSO-*d*$_6$) δ = 8.74 (s, 1H), 4.94-4.87 (m, 1H), 3.86 (s, 3H), 2.94 (dd, *J* = 12.0 Hz, 8.0 Hz, 1H), 2.75 (dd, *J* = 12.0 Hz, 4.0 Hz, 1H), 2.49-2.42 (m, 1H), 2.33-2.27 (m, 1H), 2.24-2.09 (m, 2H), 2.01-1.93 (m, 1H), 1.77-1.66 (m, 1H) ppm; $^{13}$C NMR (100 MHz, DMSO-*d*$_6$): δ = 206.8, 159.8, 153.6, 144.7, 57.6, 52.1, 46.3, 30.3, 20.9 ppm; HRMS (EI-QTOF, [M + H]$^+$): calculated for $C_{10}H_{14}N_3O_3$: 224.1035; found: 224.1032.

**3-(1*H*-Indazol-1-yl)cyclohexanone (3ag)**[12] (Scheme 3): Brown liquid; $R_f$ = 0.60 ($SiO_2$, Hexane/EtOAc = 8:2); purification system: CombiFlash MPLC (Hexane/EtOAc = 80:20); $^1$H NMR (400 MHz, $CDCl_3$) δ = 8.02 (s, 1H), 7.73 (d, *J* = 8.0 Hz, 1H), 7.41-7.36 (m, 2H), 7.62 (dt, *J* = 8.6 Hz, 1H), 4.91-4.84 (m, 1H), 3.18 (dd, *J* = 12.0 Hz, 8.0 Hz, 1H), 2.79 (dd, *J* = 12.0 Hz, 4.0 Hz, 1H), 2.51-2.47 (m, 2H), 2.41-2.31 (m, 1H), 2.25-2.18 (m, 1H), 2.14-2.05 (m, 1H), 1.83-1.71 (m, 1H) ppm; $^{13}$C NMR (100 MHz, $CDCl_3$): δ = 208.3, 138.6, 133.3, 126.3, 124.0, 121.2, 121.1, 120.8, 108.5, 56.1, 47.1, 40.7, 30.8, 21.9 ppm; HRMS (EI-QTOF, [M + H]$^+$): calculated for $C_{13}H_{15}N_2O$: 215.1184; found: 215.1180.

**Methyl 1-(3-oxocyclohexyl)-1*H*-indazole-3-carboxylate (3ah)**[12] (Scheme 3): Pale yellow solid; $R_f$ = 0.55 ($SiO_2$, Hexane/EtOAc = 8:2); purification system: CombiFlash MPLC (Hexane/EtOAc = 80:20); mp = 90-92 °C (Lit[1] mp = 91.8-92.6 °C); $^1$H NMR (400 MHz, $CDCl_3$) δ = 8.23 (d, *J* = 8.0 Hz, 1H), 7.49-7.43 (m, 2H), 7.33 (dt, *J* = 8.0 Hz, 1H), 4.91-4.84 (m, 1H), 4.03 (s, 3H), 3.30 (t, *J* = 12.0 Hz, 1H), 2.83 (dd, *J* = 12.0 Hz, 4 Hz, 1H), 2.56-2.43 (m, 3H), 2.30-2.16 (m, 2H), 1.84-1.73 (m, 1H) ppm; $^{13}$C NMR (100 MHz,

$CDCl_3$): δ = 207.5, 162.9, 139.7, 135.3, 127.0, 123.7, 123.4, 122.4, 109.1, 52.2, 52.1, 47.2, 40.5, 30.9, 22.1 ppm; HRMS (EI-QTOF, $[M + H]^+$): calculated for $C_{15}H_{17}N_2O_3$: 273.1239; found: 273.1236.

**3-(4-Bromo-1*H*-indazol-1-yl)cyclohexanone (3ai)**[12] (Scheme 3): Brown solid; $R_f$ = 0.6 ($SiO_2$, Hexane/EtOAc = 8:2); purification system: CombiFlash MPLC (Hexane/EtOAc = 80:20); mp = 89-90 °C (Lit[1] mp = 87.1-88.0 °C); $^1$H NMR (400 MHz, $CDCl_3$) δ = 8.02 (s, 1H), 7.35-7.30 (m, 2H), 7.22 (t, *J* = 8.0 Hz, 1H), 4.86-4.79 (m, 1H), 3.17 (dd, *J* = 12.0 Hz, 8.0 Hz, 1H), 2.78 (dd, *J* = 12 Hz, 4.0 Hz 1H), 2.51-2.47 (m, 2H), 2.42-2.31 (m, 1H), 2.25-2.18 (m, 1H), 2.15-2.07 (m, 1H), 1.85-1.71 (m, 1H) ppm; $^{13}$C NMR (100 MHz, $CDCl_3$): δ = 207.9, 139.1, 133.5, 127.1, 125.1, 123.7, 114.8, 107.6, 56.6, 47.06, 40.6, 30.8, 21.8 ppm; HRMS (EI-QTOF, $[M + H]^+$): calculated for $C_{13}H_{14}BrN_2O$: 293.0289; found: 293.0285.

**3-(1*H*-Pyrazol-1-yl)cyclopentanone (3ba)**[12] (Scheme 4): Pale brown sticky liquid; $R_f$ = 0.60 ($SiO_2$, Hexane/EtOAc = 8:2); purification system: CombiFlash MPLC (Hexane/EtOAc = 80:20); $^1$H NMR (400 MHz, $CDCl_3$) δ = 7.53 (d, *J* = 3.2 Hz, 1H), 7.44 (d, *J* = 4.0 Hz, 1H), 6.26 (t, *J* = 4.0 Hz, 1H), 4.99-4.93 (m, 1H), 2.86-2.69 (m, 2H), 2.65-2.39 (m, 2H), 2.36-2.27 (m, 1H) ppm; $^{13}$C NMR (100 MHz, $CDCl_3$): δ = 215.1, 139.6, 127.9, 105.6, 58.5, 44.7, 36.9, 30.3 ppm; HRMS (EI-QTOF, $[M + H]^+$): calculated for $C_8H_{11}N_2O$: 151.0871; found: 151.0866.

**3-(1*H*-Indazol-1-yl)cyclopentanone (3bg)**[12] (Scheme 4): Brown sticky liquid; $R_f$ = 0.60 ($SiO_2$, Hexane/EtOAc = 8:2); purification system: CombiFlash MPLC (Hexane/EtOAc = 80:20); $^1$H NMR (400 MHz, $CDCl_3$) δ = 7.99 (s, 1H), 7.74 (d, *J* = 8.0 Hz, 1H), 7.46-7.38 (m, 2H), 7.17 (t, *J* = 8.6 Hz, 1H), 5.34-5.28 (m, 1H), 2.97 (dd, *J* = 16.0 Hz, 4.0 Hz, 1H), 2.77 (dd, *J* = 20.0 Hz, 8.0 Hz, 1H), 2.71-2.62 (m, 1H), 2.58-2.47 (m, 2H), 2.40-2.32 (m, 1H) ppm; $^{13}$C NMR (100 MHz, $CDCl_3$): δ = 215.6, 139.0, 133.3, 126.3, 124.3, 121.3, 120.8, 108.6, 55.0, 44.1, 36.7, 29.6 ppm; HRMS (EI-QTOF, $[M + H]^+$): calculated for $C_{12}H_{13}N_2O$: 201.1027; found: 201.1022.

**3-(1*H*-Pyrazol-1-yl)cycloheptanone (3ca)**[12] (Scheme 4): Sticky liquid; $R_f$ = 0.60 ($SiO_2$, Hexane/EtOAc = 8:2); purification system: CombiFlash MPLC (Hexane/EtOAc = 80:20); $^1$H NMR (400 MHz, $CDCl_3$) δ = 7.50 (d, *J* = 3.2 Hz, 1H), 7.38 (d, *J* = 3.8 Hz, 1H), 6.24 (t, *J* = 4.0 Hz, 1H), 4.48 (tt, *J* = 12.0 Hz, 1H), 3.28 (dd, *J* = 16.0 Hz, 12.0 Hz, 1H), 2.85 (td, *J* = 8.0 Hz, 1H), 2.67-2.6 (m, 1H), 2.55-2.48 (m, 1H), 2.27-2.12 (m, 2H), 2.07-1.94 (m, 1H), 1.82-1.72 (m, 2H), 1.61-1.51 (m, 1H) ppm; $^{13}$C NMR (100 MHz, $CDCl_3$): δ = 210.4, 139.1, 127.1, 105.4, 58.7, 50.2, 44.0, 37.7, 26.5, 23.6 ppm; HRMS (EI-QTOF, $[M + H]^+$): calculated for $C_{10}H_{15}N_2O$: 179.1184; found: 179.1180.

**3-(1*H*-Indazol-1-yl)cycloheptanone (3cg)**[12] (Scheme 4): Pale yellow Solid; $R_f$ = 0.60 ($SiO_2$, Hexane/EtOAc = 8:2); purification system: CombiFlash MPLC (Hexane/EtOAc = 80:20); mp = 93-95 °C (Lit[1] mp = 91.4 - 92.4 °C); $^1$H NMR (400 MHz, $CDCl_3$) δ = 7.90 (s, 1H), 7.69 (d, *J* = 8.0 Hz, 1H), 7.63 (d, *J* = 8.0 Hz, 1H), 7.27 (t, *J* = 8.0 Hz, 1H), 7.07 (t, *J* = 8.0 Hz, 1H), 4.76-4.68 (m, 1H), 3.45 (dd, *J* = 16.0 Hz, 12.0 Hz, 1H), 2.94 (dd, *J* = 12.0 Hz, 4.0 Hz, 1H), 2.81-2.64 (m, 1H), 2.58-2.5 (m, 1H), 2.36-2.31 (m,

2H), 2.12-1.97 (m, 2H), 1.86-1.75 (m, 1H), 1.64-1.53 (m, 1H) ppm; $^{13}$C NMR (100 MHz, $CDCl_3$): δ = 209.7, 148.6, 126.0, 121.7, 121.4, 120.7, 120.1, 117.4, 60.5, 50.4, 44.0, 38.2, 26.6, 23.6 ppm; HRMS (EI-QTOF, $[M + H]^+$): calculated for $C_{14}H_{17}N_2O$: 229.1340; found: 229.1331.

**Methyl 1-(3-oxocycloheptyl)-1*H*-indazole-3-carboxylate (3ch)**[12] (Scheme 4): Grey solid; $R_f$ = 0.6 ($SiO_2$, Hexane/EtOAc = 8:2); purification system: CombiFlash MPLC (Hexane/EtOAc = 80:20); mp = 92-95 °C (Lit[1] mp = 95.4-96.2 °C); $^1$H NMR (400 MHz, $CDCl_3$) δ = 8.01 (d, *J* = 8.0 Hz, 1H), 7.77 (d, *J* = 8.0 Hz, 1H), 7.35 (t, *J* = 8.0 Hz, 1H), 7.28 (t, *J* = 8.0 Hz, 1H), 6.05-5.98 (m, 1H), 4.03 (s, 3H), 3.52 (dd, *J* = 16.0 Hz, 12.0 Hz, 1H), 2.91 (dd, *J* = 12.0 Hz, 4.0 Hz, 1H), 2.76-2.59 (m, 2H), 2.37-2.3 (m, 2H), 2.1-1.98 (m, 2H), 1.87-1.76 (m, 1H), 1.74-1.64 (m, 1H) ppm; $^{13}$C NMR (100 MHz, $CDCl_3$): δ = 210.2, 160.7, 147.4, 126.3, 125.2, 123.2, 122.7, 121.4, 118.3, 58.3, 52.0, 50.2, 44.1, 38.2, 27.0, 23.9 ppm; HRMS (EI-QTOF, $[M + H]^+$): calculated for $C_{16}H_{19}N_2O_3$: 287.1395; found: 287.1392.

**4-(1*H*-Indazol-1-yl)butan-2-one (3dg)**[12] (Scheme 4): Pale yellow stick liquid; $R_f$ = 0.40 ($SiO_2$, Hexane/EtOAc = 8:2); purification system: CombiFlash MPLC (Hexane/EtOAc = 80:20); $^1$H NMR (400 MHz, $CDCl_3$) δ = 7.97 (s, 1H), 7.65 (d, *J* = 8.0 Hz, 1H), 7.62 (d, *J* = 8.0 Hz, 1H), 7.26 (t, *J* = 8.0 Hz, 1H), 7.05 (t, *J* = 8.0 Hz, 1H), 4.67 (t, *J* = 8.0 Hz, 2H), 3.19 (t, *J* = 8.0 Hz, 2H), 2.13 (s, 3H) ppm; $^{13}$C NMR (100 MHz, $CDCl_3$): δ = 205.5, 149.0, 125.9, 123.8, 121.5, 120.2, 117.1, 47.6, 43.3, 30.1 ppm; HRMS (EI-QTOF, $[M + H]^+$): calculated for $C_{11}H_{13}N_2O$: 189.1027; found: 189.1023.

## ACKNOWLEDGEMENTS

CCM appreciates Science and Engineering Research Board (SERB), New Delhi for financial support in the form of research grants (CRG/2020/004509 and ECR/2016/000337). The authors extend their appreciation to the Researchers Supporting Project number (RSP2023R396), King Saud University, Riyadh, Saudi Arabia.

## REFERENCES

1. (a) L. Zhong, Y. Li, L. Xiong, W. Wang, M. Wu, T. Yuan, W. Yang, C. Tian, Z. Miao, T. Wang, and S. Yang, *Signal Transduct. Target. Ther.*, 2021, **6**, 201; (b) M. A. S. Abourehab, A. M. Alqahtani, B. G. M. Youssif, and A. M. Gouda, *Molecules*, 2021, **26**, 6677; (c) J. Real, M. C. Serna, M. Giner-Soriano, R. Forés, G. Pera, E. Ribes, M. Alzamora, J. R. Marsal, A. Heras, and R. Morros, *BMC Cardiovasc. Disord.*, 2018, **18**, 1; (d) H. D. Venkatesh, S. V. Tadas, C. O. N. Vincent, G. K. Lalji, K. Ritesh, C. Pankaj, N. Donnell, F. Rena, G. Zhiyong, Q. Yun, and M. H. B. Angela, *J. Med. Chem.*, 2005, **48**, 2972; (e) C. Jorand-Lebrun, S. Crosignani, J. Dorbais, T. Grippi-Vallotton, and A. Pretre, WO 2012/084704Al, 28 June, 2012.
2. (a) J. Moran, P. Dornan, and A. M. Beauchemin, *Org. Lett.*, 2007, **9**, 3893 and references cited there

in; (b) A. Gurjar, "*Michael addition of some amines experimental and theoretical investigation*" Ph.D Thesis, The IIS University, 20 November, 2017, http://hdl.handle.net/10603/183715.

3. (a) Z. Galeštoková and R. Šebesta, *Eur. J. Org. Chem.*, 2012, 6688; (b) S. U. Dighe, R. Mahar, S. K. Shukla, R. Kant, K. Srivastava, and S. Batra, *J. Org. Chem.*, 2016, **81**, 4751; (c) S. Bhattacharjee, A. A. Shaikh, and W.-S. Ahn, *Catal. Letters*, 2021, **151**, 2011.
4. (a) O. Obulesu, V. Murugesh, B. Harish, and S. Suresh, *J. Org. Chem.*, 2018, **83**, 6454; (b) Z. Li, A. Yang, X. Ma, and Z. Liu, *J. Chem. Res.*, 2020, **44**, 97; (c) M. R. Saidi, N. Azizi, E. Akbari, and F. Ebrahimi, *J. Mol. Catal. A - Chem.*, 2008, **292**, 44; (d) B. E. Uno, K. K. Deibler, C. Villa, A. Raghuraman, and K. A. Scheidt, *Adv. Synth. Catal.*, 2018, **360**, 1719.
5. (a) J. Yang, Y. Bao, H. Zhou, T. Li, N. Li, and Z. Li, *Synthesis*, 2016, **48**, 1139; (b) F.-F. Xu, L.-Y. Chen, P. Sun, Y. Lv, Y.-X. Zhang, J.-Y. Li, X. Yin, and Y. Li, *Chirality*, 2020, **32**, 378; (c) A. Talukdar and D. C. Deka, *SN Appl. Sci.*, 2020, **2**, 599.
6. (a) M. L. Kantam, M. Roy, S. Roy, M. S. Subhas, B. Sreedhar, B. M. Choudary, and R. L. De, *J. Mol. Catal. A - Chem.*, 2007, **265**, 244; (b) V. Polshettiwar and R. S. Varma, *Tetrahedron Lett.*, 2007, **48**, 8735.
7. (a) A. V. Narsaiah, *Lett. Org. Chem.*, 2007, **4**, 462; (b) J. S. Yadav, A. R. Reddy, Y. G. Rao, A. V. Narsaiah, and B. V. S. Reddy, *Synthesis*, 2007, 3447; (c) N. Azizi, R. Baghi, H. Ghafuri, M. Bolourtchian, and M. Hashemi, *Synlett*, 2010, 379; (d) N. Azizi and M. R Saidi, *Tetrahedron*, 2004, **60**, 383.
8. V. B. Labade, S. S. Pawar, and M. S. Shingare, *Monatsh. Chem.*, 2011, **142**, 1055.
9. (a) J. Zhang, C. Wang, C. Wang, W. Shang, B. Xiao, S. Duan, F. Li, L. Wang, and P. Chen, *J. Chem. Technol. Biotechnol.*, 2019, **94**, 3981; (b) S. Dutt, V. Goel, N. Garg, D. Choudhury, D. Mallick, and V. Tyagi, *Adv. Synth. Catal.*, 2020, **362**, 858.
10. (a) J. Wang, P.-F. Li, S. H. Chan, A. S. C. Chan, and F. Y. Kwong, *Tetrahedron Lett.*, 2012, **53**, 2887; (b) K. Kodolitsch, F. Gobec, and C. Slugovc, *Eur. J. Org. Chem.*, 2020, 2973 and references cited there in.
11. (a) M. I. Uddin, K. Nakano, Y. Ichikawa, and H. Kotsuki, *Synlett*, 2008, 1402; (b) X.-J. Du, Z.-P. Wang, Y.-L. Hou, C. Zhang, Z.-M. Li, and W.-G. Zhao, *Tetrahedron Lett.*, 2014, **55**, 1002; (c) G. Bosica and A. J. Debono, *Tetrahedron*, 2014, **70**, 6607.
12. S. Polina, V. P. R. K. Putta, R. Gujjarappa, P. P. Pujar, and C. C. Malakar, *J. Heterocycl. Chem.*, 2021, **58**, 1029.
13. (a) A. K. Kabi, R. Gujjarappa, N. Vodnala, D. Kaldhi, U. Tyagi, K. Mukherjee, and C. C. Malakar, *Tetrahedron Lett.*, 2020, **61**, 152535; (b) S. Qiao, N. Zhang, H. Wu, and M. Hanas, *Synth. Commun.*, 2021, **51**, 2873.

14. (a) V. P. R. K. Putta, R. Gujjarappa, U. Tyagi, P. P. Pujar, and C. C. Malakar, *Org. Biomol. Chem.*, 2019, **17**, 2516; (b) V. P. R. K. Putta, N. Vodnala, R. Gujjarappa, U. Tyagi, A. Garg. S. Gupta, P. P. Pujar, and C. C. Malakar, *J. Org. Chem.*, 2020, **85**, 380 and references cited there in.